

# PLANETESIMAL ACCRETION IN BINARY SYSTEMS: THE EFFECTS OF GAS DISSIPATION

Ji-Wei Xie and Ji-Lin Zhou

*Department of Astronomy, Nanjing University, Nanjing 210093, China*

xjw0809@163.com

## ABSTRACT

Currently, one of major problems concerning planet formation theory in close binary systems is, the strong perturbation from the companion star can increase relative velocities ( $\Delta V$ ) of planetesimals around the primary and thus hinder their growth. According to previous studies, while gas drag can reduce the  $\Delta V$  between bodies of the same sizes by forcing orbital alignment to planetesimals, it increases the  $\Delta V$  among bodies of different sizes. In this paper, focusing on the  $\gamma$  Cephei binary system, we propose a mechanism that can overcome this difficulty. We show that in a dissipating gas disk (with a typical dissipating timescale of  $\sim 10^5 - 10^6$  years), all the planetesimals eventually converge towards the same forced orbits regardless of their sizes, leading to much lower impact velocities among them. These  $\Delta V$  decrease processes progressively increase net mass accretion and even trigger runaway growth for large bodies (radius  $> 15$  km). The effect of size distribution of planetesimals is discussed, and found to be one of the dominant factors that determine the outcome of collisional evolution. Anyway, it can be concluded that by including the gas dissipation in the early stage of disk evolution, the conditions for planetesimal accretion become much better, and the process from planetesimal to planet-embryo can be carried out in close binary systems like  $\gamma$  Cephei.

*Subject headings:* methods: numerical — planetary systems: formation

## 1. INTRODUCTION

With the increasing number of discovered planets in binary systems and the belief that a majority of solar-type stars reside in binary or multiple systems, problem of planetary formation in binary systems becomes a crucial one. Most of discovered planet-bearing binary

systems are S-type systems (e.g.  $\gamma$  Cephei system, see Hatzes et al. 2003) in which planets orbit the primary star with a companion star surrounding them on an outer orbit. According to the classical planetary formation scenario, planets form in a protoplanetary disk of gas and dust orbiting a protostar. The formation process is usually treated in three stages (Lissauer 1993; Papaloizou & Terquem 2006; Armitage 2007): [S1.] formation of kilometer-size planetesimals ( $10^{18} - 10^{22}$  g) from sticking collisions of dust (Weidenschilling & Cuzzi 1993) or from gravitational fragmentation of a dense particle sub-disk near the midplane of the protoplanetary disk (Goldreich & Ward 1973) on timescales of the order of  $10^4$  years, [S2.] accretion of planetesimals into planetary embryos ( $10^{26} - 10^{27}$  g, Mercury- to Mars-size) through a phase of “runaway” and “oligarchic” growth on a timescale of the order of  $10^4 - 10^5$  years, depending on initial planetesimal sizes, duration of the runaway growth period, possible transition to oligarchic mode (Greenberg et al. 1978; Wetherill & Stewart 1989; Barge & Pellat 1993; Kokubo & Ida 1996, 1998, 2000; Rafikov 2003, 2004). [S3.] giant impacts between embryos, producing full-size ( $10^{27}$  to  $10^{28}$  g) terrestrial planets in about  $10^7 - 10^8$  years (Chambers & Wetherill 1998; Kokubo, Kominami & Ida 2006; Levison & Agnor 2003). Here we focus on the stage II to see the influence of the companion on the planetesimal accretion.

The companion star, especially when it is on a close orbit with a high eccentricity, may prevent planetary formation through reducing the size of the accretion disk (Artymowicz & Lubow 1994), and exciting high relative velocities between colliding planetesimals (Heppenheimer 1978; Whitmire et al. 1998). The relative velocity ( $\Delta V$ ) is a critical parameter, which determines whether accretion or erosion dominates. Due to the perturbation by the companion,  $\Delta V$  may exceed the planetesimal escape velocity ( $V_{esc} \sim 100 \times (R_p/100km) \text{ m s}^{-1}$ ), and thus inhibit runaway growth. Furthermore,  $\Delta V$  can even exceed the threshold velocity ( $V_{ero}$ ) for which erosion dominates accretion. Here  $V_{ero}$  is a few times larger than  $V_{esc}$ , depending on the prescription on collision.

Since planetesimals orbit the star in a sub-Keplerian gas disk (Adachi et al. 1976), the presence of gas drag does not only damp the companion’s secular perturbation, but it also forces a strong periastron alignment of planetesimal orbits. This alignment significantly reduces  $\Delta V$  between equal-sized bodies, favoring the accretion process (Marzari & Scholl 2000). Nevertheless, the alignment forced by the gas drag induces another problem. As the alignment is size-dependent, it can only reduce  $\Delta V$  between planetesimals of the same sizes, and at the same time it increases  $\Delta V$  between planetesimals of different sizes. Thebault et al. (2006) find that this differential orbital alignment is very efficient, leading to a significant  $\Delta V$  increase for any departure from the exact equal-size condition ( $R_1 = R_2$ , where  $R_1$  and  $R_2$  are the radiuses of the two colliding bodies).

Pervious studies adopted a steady gas disk in which dissipating process was neglected and the local gas density was constant. This assumption, which is valid only when the planetesimal accretion time scale (of the order of  $10^4$  to  $10^5$  years) is much shorter than the dissipating time scale of local gas density, is violated under the following conditions. 1)When the disk viscosity is high or photoevaporation from external star exists (Hollenbach et al. 1994, 2000; Matsuyama et al. 2003), disks can dissipate very fast and have short lifetimes within a few  $10^5$  years. 2)It is suggested that the assumption of a single time scale for disk dissipation is not correct, and there could be a wide spread of disk lifetimes, with a large fraction of short-lived disks (Bouwman et al. 2006). As calculated by Matsuyama et al.(2003) and Alexander et al. (2006b), even for a disk with a lifetime of the order of  $10^6$  years, local density can decrease by as many as two orders of magnitude within the first few  $10^5$  years. For these two considerations, therefore, a model that includes gas dissipation is essential for studying planetesimal accretion.

In this paper, we consider a model in which gas density progressively decreases, to see how the conditions of planetesimal accretion are affected by the gas dissipating process. As expected, the planetesimal growth conditions change to being accretion-friendly due to an dissipation induced orbital convergence, which reduces  $\Delta V$  between bodies of different sizes. We describe our numerical model and methods in section 2. In section 3, first, we simply review the planetesimal dynamics under the coupled influence of secular perturbation and gas drag, and then present the results. Some related and crucial issues, such as the radial drift, impact rate, erosion conditions and remanent gas, are discussed in section 4. Finally, in section 5, we summarize this paper.

## 2. NUMERICAL MODEL AND METHODS

### 2.1. Gas Disk Model

We made the gas model similar to that of Thebault et al. (2004). Following Weiden-schilling and Davis (1985), the gas drag can be expressed as:

$$\mathbf{F} = -Kv\mathbf{v}, \quad (1)$$

where  $\mathbf{F}$  is the force per unit mass,  $\mathbf{v}$  the relative velocity between the planetesimal and gas,  $v$  the velocity modulus, and  $K$  is the drag parameter defined as:

$$K = \frac{3\rho_g C_d}{8\rho_p R_p}, \quad (2)$$

$$\rho_g = \rho_{g0} T^{-n}, T = \frac{t}{T_s + 1}, \quad (3)$$

where  $\rho_g$  is the local gas density with an initial value of  $\rho_{g0}$ ,  $\rho_p$  and  $R_p$  the planetesimal density and radius, respectively.  $C_d$  is a dimensionless coefficient related to the shape of the body ( $\simeq 0.4$  for spherical bodies). The  $T^{-n}$  function, in which time  $T$  is scaled by  $T_s$ , is used to include the gas dissipation, and it is based on the analytic similar solutions given by Lynden-Bell and Pringle (1974). Taking typical parameters from Hartmann et al. (1998), where  $n = 3/2$ ,  $T_s = 10^5$  years, we plot figure 1 to show the gas disk density evolution vs. time. The gas disk is scaled by the Minimum Mass solar Nebula (hereafter MMN for short) and has the same profile to the MMN (Hayashi 1981). The initial gas density is 10 MMN, and the corresponding disk mass is about 100 Jupiter mass. As shown in figure 1, gas density rapidly decreases from 10 MMN to 0.5 MMN within the first few  $10^5$  years, and then it experiences a slow damping process lasting for a few million years. This dissipation model is consistent with current theoretic calculations (Matsuyama et al. 2003; Alexander et al. 2006a, 2006b) and observations (Strom et al. 1993; Haisch et al. 2001; Chen & Kamp 2004), which suggest a typical disk age of 1 million years with a large scatter from 0.1 to 10 million years. Notice that the effects of binarity on the dissipation of gas disk are not taken into account because details of these issues are poorly known at present.

Our model implicitly assumes an axisymmetric gas disk with constant circular streamlines and follows a classical Hayashi (1981) power law distribution. We are aware that this is a crude simplification for modeling gas disk in close binary systems. In reality, the gas disk around the primary also “feels” the companion’s perturbation, under which disk structure would vary from the simplified gas model. For example, the companion’s perturbation can induce spiral structures within the disk (Artymowicz and Lubow, 1994). To fully model the behavior of planetesimals in these complex gas disks, one would probably have to rely on hydro-code modeling of the gas in addition to N-body type models for planetesimals. Such an all-encompassing gas plus planetesimals modeling goes beyond the scope of our study in this paper, and it is certainly the direction of further binary disk studies. Therefore, taking a first step here, we just prefer a simplified approach where gas drag force is given by equation (1). As discussed by some previous studies (Scholl et al. 2007, Thebault et al. 2006), this kind of simplification, on the average, is reasonable at least for the dynamical evolution of kilometer-size planetesimals.

## 2.2. Initial Conditions

We focus on the  $\gamma$  Cephei system, which is a close S-type binary planetary system, hence being a good example to test the influence of the companion on planetesimal accretion. Most parameters adopted in this paper are listed in table 1. The initial gas disk has the same profile to MMN, but is denser by 10 times. We concentrate on planetesimals of four radiuses ( $R_p = 2.5, 5, 15, 50$  km). As stated by Thebault et al. (2006), for impacts between small bodies ( $1 < R_p < 10$  km), the delivered kinetic energy peaks at roughly  $R_1 \simeq 1/2R_2$ , where  $R_1$  and  $R_2$  are the radiuses of the two colliding bodies. For the bigger ones, this  $R_1/R_2$  ratio is somewhat smaller. Hence, the relative velocity  $\Delta V(2.5, 5)$  between bodies of  $R_p = 2.5$  km and  $R_p = 5$  km can be typical example values for small planetesimals, and  $\Delta V(15, 50)$  for large ones. All the planetesimals initially have very small inclinations based on the work of Hale (1994), which suggests that approximate coplanarity between the equatorial and orbital planes exist for solar-type binary systems with separations less than 30-40 AU. Since it is unrealistic that all planetesimals form synchronously, some earlier formed planetesimals may have been pumped up to eccentric orbits while some others have just formed. For this reason, the initial planetesimal orbits should have random eccentricities within the range from 0 to  $e_{max}$ , where  $e_{max}$  is the maximum eccentricity that pumped up by the companion. In the  $\gamma$  Cephei system,  $e_{max}$  is about 0.1 at 2 AU from the primary.

One implicit initial condition in this paper is that, of course, kilometer-size planetesimals have already formed when the disk begins dissipating. At present, with the poor knowledge on planetesimal formation in binary systems, whether this assumption is valid or not is not for sure at all. According to current limited knowledge on planetesimal formation around a single star, kilometer-size planetesimal can form within  $10^3 - 10^5$  years through sticking collision or by gravitational instability after dust having settled down on the mid-plane (Lissauer 1993; Weidenschilling 1997; Goldreich & Ward 1973; Youdin & Shu 2002). In such case, the timescale of planetesimal formation can be much shorter than that of gas disk dissipation (about  $10^6$  years is considered in this paper), and thus it is reasonable to assume that the gas dissipation starts when a population of kilometer-size planetesimals exist in the system.

## 2.3. Numerical Methods

We performed two kinds of runs. First, we numerically integrated the equations of motion for 1000 independent planetesimals with semi-major axes from 1 to 4 AU. The focus is put on the time-evolution of orbital eccentricities and of orbital periastrons. Second, we concentrate on the time-evolution of  $\Delta V$  at a specific region near 2 AU from the primary

star where a planet is detected. This is the configuration of the  $\gamma$  Cephei system that we specifically consider here. Planetesimals are initially distributed in a ring near 2 AU. Since the planetesimal sizes (order of km) are very small comparing to the system typical scale (order of AU), it is very difficult to track all “real” physical impacts among these planetesimals (Brahic 1977, Charnoz et al. 2001a, 2001b; Lithwick & Chiang 2007, etc). In such case, we have to resort to the classical “inflated radius” assumption, which assumes an artificially increased radius to each particle (e.g. Brahic 1977; Thebault & Brahic 1998; Marzari & Scholl 2000). For planetesimals considered here, an artificially increased radius (about  $10^{-5} - 10^{-4}$  AU) of 100 times larger than the “real” radius is adopted for each planetesimal.

In all the runs, we used the fourth order Hermite integrator (Kokubo et al. 1998), including the gas drag force and the perturbation of companion. As gas drag also forces inward drift of planetesimals, we adopt following boundary conditions: bodies whose semi-major axes are less than  $R_{in}$  (greater than  $R_{out}$ ), will be reset to  $R_{out}$  ( $R_{in}$ ), where  $R_{in}$  and  $R_{out}$  are the inner and outer boundaries of planetesimal belt, respectively. In these resetting processes, only the semi-major axes of those bodies are changed, while other orbital elements are preserved.

### 3. RESULTS

#### 3.1. Planetesimal Dynamics: the Secular Approximation

Before presenting the results, let’s review the planetesimal dynamics in a perturbed system. Heppenheimer (1978) developed a simplified theory for the evolution of planetesimal eccentricity with time in binary systems. First, he defined two variables  $h$  and  $k$  as

$$h = e_p \sin(\varpi), k = e_p \cos(\varpi), \quad (4)$$

where  $e_p$  is the planetesimal eccentricity and  $\varpi$  its periastron longitude defined with respect to that of the companion star ( $\varpi = \varpi_p - \varpi_B$ , where  $\varpi_p$  and  $\varpi_B$  are the periastron longitudes of the companion and the planetesimal, respectively). Then, introducing in the Langrange planetary equations, he obtained the following equations for  $h$  and  $k$ :

$$\frac{dh}{dt} = Ak - B, \quad (5)$$

$$\frac{dk}{dt} = -Ah, \quad (6)$$

where the constants  $A$ ,  $B$  are

$$A = \frac{3}{4} \frac{M_A}{n(1 - e_B^{3/2})}, B = \frac{15}{16} \frac{ae_B}{n(1 - e_B^{5/2})}, \quad (7)$$

with  $e_B$  the eccentricity of the binary system and  $M_A$  the mass of the primary star.  $a$  and  $n$  are the semi-major axis and mean motion of the planetesimal, respectively. The units of mass, distance, and time are normalized in such a way that the gravitational constant  $G$  and the sum of the masses of the two stars are set equal to 1. The semimajor axis of the binary  $a_B$  is chosen as the units of length, so that the time is expressed in units of  $(1/2\pi)T_B$ , where  $T_B$  is the orbital period of the binary system.

In  $h - k$  plane, there is an equilibrium point (where  $dh/dt = 0, dk/dt = 0$ ) for equations (5) and (6), which is referred to as E0 in this paper. At E0,  $e_p = e_f$  and  $\varpi_p = \varpi_f = \varpi_B$ , where  $e_f = B/A$  and  $\varpi_f = \varpi_B$  are the forced eccentricity and periastron of the planetesimal respectively. If a planetesimal reaches the equilibrium point E0, its eccentricity and periastron will fix on  $B/A$  and  $\varpi_B$  forever.

To compute the effect of gas drag on the variables  $h$  and  $k$ , Marzari and Scholl (2000) modified equations (5) and (6) as following:

$$\frac{dh}{dt} = Ak - B - Dh(h^2 + k^2)^{1/2}, \quad (8)$$

$$\frac{dk}{dt} = -Ah - Dk(h^2 + k^2)^{1/2}, \quad (9)$$

where  $D$  is a coefficient to measure the gas drag force. According to these equations, for a specific  $D$ , the planetesimal orbit will quickly or slowly (depending on the  $D$  value, a larger value  $D$  leads to a faster speed) reaches another equilibrium point(different with E0), with an equilibrium eccentricity below  $B/A$ . Furthermore, AND THIS IS THE CRUCIAL POINT OF THIS STUDY, if  $D$  damps slowly(caused by gas dissipation), planetesimals will shift their orbits from this equilibrium point eventually toward E0.

In figure 2, we illustrate these processes. In no gas case, the motion in the  $h - k$  plane is circulating around the equilibrium point  $E0$  that derived from equations (5) and (6). For the case with gas drag in our gas disk model, motions are divided into the following two phases: a) “no dissipation phase” in the first few  $10^3$  years, in which gas disk dose not significantly dissipate and planetesimals of different sizes quickly reach different equilibrium points depending on their sizes(point  $E1$  for bodies of 50 km,  $E2$  for 20 km, see figure 2), b) “dissipating phase”, in which gas disk gradually dissipates, at the same time all the motions shift along the line  $E4 - E0$ , and eventually fix on the same equilibrium point  $E0$  regardless

of their sizes. We also analyze the effects of initial orbits on the dynamical behavior. As shown in figure 2, bodies with the same sizes(5 km) but different initial orbits (one is at  $I1$ , the other is at  $I2$ ) go through different paths( $I1 - E4$ ,  $I2 - E4$ ) to reach the same equilibrium point( $E4$ ). After that, they both experience the same “dissipating phase” from  $E4$  to  $E0$ . From this point, we can see that how to choose the initial planetesimal orbits do not affect the final results which are based primarily on the latter “dissipating phase”.

The appearance of the dissipating phase and the dynamical behavior of planetesimal orbits during this phase are very important because they provide channels to reduce the differential phasing effect induced by the size-dependence of gas drag. Based on the above theoretical analysis, we can expect a relative velocity( $\Delta V$ ) decrease from the convergence of all the planetesimal orbits. In the next two subsections, we will numerically simulate this  $\Delta V$  decrease process.

### 3.2. Time-evolution of Eccentricity and Periastron

We first performed a simulation in which 1000 planetesimals (4 equal-number groups:  $R_p = 2.5, 5, 15, 50$  km, mutual interactions were neglected) were initially distributed between 1 AU and 4 AU from the primary. Figure 3 shows the distributions of planetesimal eccentricities and periastrons vs. semi-major axes at different epoches. Beyond 3 AU, the distributions of planetesimal eccentricities and periastrons are random because the shorter period perturbation and mean motion resonances are dominant there. Thus, hereafter only planetesimals within 3 AU are discussed. In figure 3a(or b), every eccentricity (or periastron) reaches an equilibrium value at 5,000 years. These equilibrium values, as discussed in the above subsection and also pointed out by previous studies(Thebault et al. 2006), depend on the balance between the perturbation by the companion and the gas drag force. Due to the size-dependence of gas drag force, bodies of different sizes reach different equilibrium eccentricities (or periastrons). The four lines in each panel are corresponding to bodies of four kinds of sizes ( $R_p = 2.5, 5, 15, 50$  km). As the gas dissipates gradually, the equilibrium eccentricities (or periastrons) move to larger values, but at the same time the differences among them become smaller (see Fig. 3c(or d)). After a long time (5,000,000 years, see Fig. 3e(or f)), almost all eccentricities (or periastrons) converge towards  $e_f$  ( $\varpi_f$ ).

### 3.3. Time-evolution of Relative Velocity

We perform another simulation to investigate the time-evolution of  $\Delta V$  in a specific place (at 2 AU from the primary). In this calculation, 1000 Planetesimals were initially distributed with major-axes between 1.5 and 3 AU. This planetesimal ring is wide enough that to trace most of collisions at 2AU.

The results are plotted in figure 4. Figure 4b and figure 4c show the average eccentricity and periastron of bodies at 2 AU as the functions of time, respectively. As disk gradually dissipates, all the planetesimals converge towards the same forced orbits where  $e_p = e_f$ ,  $\varpi_p = \varpi_B$  (also see E0 in figure 2). Figure 4a plots the  $\Delta V(R_1, R_2)$  as the function of time. It is evident that the larger differences in orbital elements, the larger value of  $\Delta V$ . From figure 4a, it appears that the  $\Delta V$  between bodies of equal-size are always small because of the orbital alignment. However, the  $\Delta V$  between bodies of different sizes first increase quickly to high values (e.g.  $300 \sim 800 \text{ m s}^{-1}$ ), then each of them experiences a relatively slow decrease. This  $\Delta V$  decrease is most efficient for large bodies. For 15 km-size and 50 km-size bodies, the relative velocity  $\Delta V(15, 50) \sim 300 \text{ m s}^{-1}$  is much larger than their escape velocities  $V_{esc} \sim 50 \text{ m s}^{-1}$  at the beginning. After about  $3 \times 10^5$  years,  $\Delta V(15, 50)$  get lower (about  $40 \text{ m s}^{-1}$ ) than the escape velocities of the large planetesimals, so that runaway growth can occur.

To compare with the dissipating gas drag case showed in figure 4, we perform one more case with constant gas drag. It shows, in figure 5, that without gas dissipation every  $\Delta V$  is forced on a relatively high value determined by the equilibrium between the gas drag force and secular perturbation. The main difference with the dissipating gas case is that there is no late stage with size-independent orbital phasing and thus no  $\Delta V$  decrease.

## 4. DISCUSSIONS

### 4.1. Impact Rate

As impacts of different types (between the same sizes or different sizes) have totally different  $\Delta V$  and thus different outcomes (erosion, incomplete accretion, complete accretion and runaway growth), the condition that which type of collision dominates becomes crucial for planetesimal growth. Figure 6 plots the distributions of impact rates for two cases: a) standard case, b) random case. In both cases, we compute 1000 planetesimals whose radius distribution is assumed as a gaussian function centered at 8 km with a dispersion  $\Delta R = 7$  km. The only difference between them is the companion and gas drag are not included in

the random case. As shown in figure 6, for the random case, the distribution of impact rates depends only on the initial size distribution: impacts occur more often in the places where more planetesimals are distributed for impacts between equal-sized bodies close to the center of the Gaussian. On the other hand, in the standard case, the distribution is obviously size-dependent: impacts mainly occur between bodies of different sizes. By comparing these two cases, it is clear: under the coupled effect between gas drag and the companion’s perturbation, impacts between bodies of different sizes are favored, while impacts between bodies of the same(or similar) sizes are hindered. This result can be understood in this way: for bodies of the same sizes, as they have the same forced orbits and radial drifts, one can only collide with another when their semimajors are very close; for bodies of different sizes, in contrast, as they have different forced orbits and radial drifts, one can cross many more planetesimal orbits on a much larger region.

#### 4.2. Accretion or Erosion

The key result of this paper presented in section 3 is: as gas dissipates, all planetesimals eventually converge towards the same forced orbits regardless of their sizes, leading to much lower  $\Delta V$  than in the constant-gas density case. To further see the effects of these  $\Delta V$  decreasing processes on planetesimal collisional evolution(accretion or erosion), we then perform a quantitative study.

Following Kortenkamp & Wetherill (2000), we adopt the disruption limit given by Love and Ahrens (1996), and compute the net mass accretion ratio (see Appendix for details) for every impact. Figure 7 shows the time-evolution of net mass accretion ratios( $A_r$ ) for impacts between different size groups. For impacts between bodies of the same sizes, net mass accretion ratios are not plotted, since the  $\Delta V$  are always low enough for runaway growth in such cases. As shown in figure 7, it can be summarized as following: 1) for small bodies ( $R_p < 5$  km), collisions always lead to erosion during the first  $7 \times 10^5$  years, after which accretion occurs with a progressively increasing  $A_r$ , 2) for intermediate bodies( $5 < R_p < 15$  km),  $A_r$  is initially modest(75%-80%) and will progressively increase (to 90%-95%) as the gas dissipates, 3) for large bodies ( $R_p > 15$  km),  $A_r$  is always very high( $\geq 95\%$ ), 4) for impact between a large( $R_p > 15$ ) km and a small( $R_p < 5$  km) planetesimal, while the  $\Delta V$  is high and decreases slowly(see figure 4),  $A_r$  is always high ( $\geq 95\%$ ). Therefore, to fully know the details of collisions among a swarm of planetesimals will have to require an entire information of the initial planetesimal size distribution, which is, however, not clear at all with current knowledge.

Here, for simplicity, we just perform four simplified tests assuming for the planetesimal

size distribution a gaussian and three power-law functions, respectively. For the three power law cases, planetesimals have distributions given by  $N \propto m^{-1.7}$  (Makino et al. 1998) with three radius ranges, namely 1 - 50 km, 2.5 - 50 km and 5 - 50 km. For the gaussian case, the radius distribution is assumed as the gaussian function centered at 8 km with a dispersion  $\Delta R = 7$  km. Figure 8 plots the time-evolution of the average  $\Delta V$  and  $A_r$  for these four cases. It shows, at the first few  $10^3$  years (no dissipation phase), the conditions for accretion or erosion totally depend on the initial size distribution of planetesimals. In this phase, the average  $\Delta V$  is pumped up by the size-dependence of orbital alignment, and thus the accretion is inefficient ( $A_r \sim 75\%$ ) for one power law case (5 - 50 km), dangerous ( $A_r \sim 30\%$ ) for the gaussian case and another power law case (2.5 - 50 km), and even completely suppressed for the power law case (1 - 50 km). However, after a few  $10^5$  years (gas dissipation phase), all the  $\Delta V$  get low enough and accretion is efficient ( $A_r \geq 95\%$ ) for all the cases, regardless of the initial size distribution of planetesimals. Notice that the smaller bodies we consider initially, the more time the system needs to become accretion-friendly. For the power law case with minimum size of 1 km, it indeed takes about  $6 \times 10^5$  years before accretion is efficient. As discussed in the next subsection, this long timespan can worsen the radial drift problem.

### 4.3. Radial Drift

Moving in the gas disk, planetesimals undergo a headwind by which they are forced to progressively migrate inwards (Adachi et al. 1976). In the above runs, we adopt a boundary condition described in section 2.3 to keep all the planetesimals staying in our computing zone (1.5 – 3 AU). This is reasonable only if the planetesimal disk is extended enough so that planetesimals can flow into the computing zone from the outer disk. However, theoretical calculations of binary-disk interactions predict that companions might truncate circumstellar disks at an out radius of 0.2 – 0.5 times the binary semi-major axes (Artymowicz & Lubow 1994). For  $\gamma$  Cephei system,  $a_B = 18.5$  AU, then the truncated disk size is about 3.7 – 9.3 AU. Therefore, there may be not enough material supplied from the outer disk, and it means there should be enough planetesimals staying in the computing zone for at least a few  $10^5$  years to form planets. For this reason, we performed a simulation without any boundary condition to compare the results in figure 4. We find most large bodies with  $R_p = 15$  km and  $R_p = 50$  km stay in the computing zone, having  $\Delta V$  curves similar to those in figure 4, while almost all the small bodies with sizes of  $R_p = 2.5$  km and  $R_p = 5$  km are removed by gas drag. This problem of “too fast migration” will be even worse when smaller bodies are considered, such as bodies with radiuses of 1 – 10 m. As shown in figure 8, for the power law case (1 - 50 km), there is  $6 \times 10^5$  years timespan, during which erosion dominates and thus planetesimals are transformed into small fragments which are quickly removed by inward

drift.

Actually, fast inward drift induced by gas drag is a general problem in the classical planet formation model(Lissauer 1993; Papaloizou & Terquem 2006; Armitage 2007), and several ways have been proposed to address this issue. It is possible that large planetesimals ( $R_p > 10$  km, which is big enough to overcome the inward drift) form directly via gravitational instability in a few  $10^3$  years (Goldreich & Ward 1973; Youdin & Shu 2002). In addition, radial drift may allow small bodies to pileup within the inner disk to form larger planetesimals( Youdin & Chiang 2004), and the present of turbulence in gas disk can also reduce the radial drift(Durisen et al. 2005; Haghhighipour & Boss 2003; Rice et al. 2004).

#### 4.4. Remanent Gas for gaseous Planet Formation

In addition, there should be enough remanent gas to form a massive gaseous planet, as required to fit the minimum mass ( $\sim 2$  jupiter masses) of the planet detected in the  $\gamma$  Cephei system. In this paper, for a initial gas disk of 10 MMN(about 100 Jupiter mass), after  $5 \times 10^5$  years when most  $\Delta V$  have already decreased to low enough values, the remanent gas, according to figure 1, is about 7 Jupiter masses. On the other hand, Kley and Nelson (2007) suggest that the gas accretion onto a planet will be highly efficient in the  $\gamma$  Cephei system due to the large induced planet orbital eccentricity. Their simulations indicate that it needs a gas disk with only  $\sim 3$  Jupiter masses to form a gaseous planet of  $\sim 2$  Jupiter masses. Therefore, it is possible to form a massive gaseous planet in our dissipating gas model.

### 5. SUMMARY

In this paper, focusing on the  $\gamma$  Cephei system and concentrating on planetesimal impact velocities( $\Delta V$ ), we numerically investigate the conditions for planetesimal accretion in binary systems. We extend the studies of Thebault et al. (2004, 2006) by including the effect of a dissipating gas disk. We confirm some of their results that in a gas disk without dissipation, differential orbital alignment is very efficient and increase  $\Delta V$  between bodies of different sizes to high values that significantly inhabit planetesimal growth. Furthermore, we find that by including gas dissipation, the differential phasing effect induced by the size-dependence of gas drag can be reduced. In such case, as gas density decreases, all planetesimals converge their orbits towards the same forced orbits, regardless of their sizes. This orbital convergence induced by gas dissipation is most efficient for large bodies(15 - 50 km). Within  $3 \times 10^5$  years,  $\Delta V(15, 50)$  decrease to low enough values(about  $40 \text{ m s}^{-1}$  below the escape velocities of large

bodies) for which runaway growth is able to occur.

In order to get more information of the collisional evolution, we first discuss the impact rate distribution. We find, for binary systems including gas drag, collisions between bodies of different sizes are dominant due to the differential orbital alignment and the size-dependence of the radial drift. Considering this result, our mechanism which can reduce the  $\Delta V$  between bodies of different sizes, therefore, becomes much more essential for planetesimal growth.

By defining the net mass accretion ratio( $A_r$ ), we then discuss the conditions of accretion or erosion for a swam of planetesimals with different size distributions. We find the size distribution is a very crucial factor that influences the collisional evolution. For the constant gas density case, it totally dominates the growth of planetesimals, and accretions are only efficient between equal-sized bodies in such case. On the other hand, for the dissipating gas density case, effect of size distribution is dominant only at the beginning, and after a few  $10^5$  years, accretion( or even runaway growth) is always favored, regardless of the initial size distribution of planetesimals.

Due to the companion's perturbation in a binary system, disk is truncated to a smaller one and the planetesimals undergo a much faster inward drift. These effects may induce a problem that whether enough planetesimals can remain in the planet-formation zone against the inward migration. We perform some computations for this consideration, and find most small bodies( $R_p < 10$  km) are removed within a few  $10^5$  years, while no significant influences on large bodies( $R_p > 15$  km). Furthermore, the inward drift problem will be much more acute when the initial planetesimal population is composed mainly of small bodies( $R_p < 2.5$  km). In such case, erosion dominates for the first few  $10^5$  years, and planetesimals are transformed into small fragments which are quickly removed by inward drift.

Finally, we estimate the remanent gas for forming a gaseous planet. In our dissipating gas disk model, after  $5 \times 10^5$  when  $\Delta V$  among most of planetesimals have already decreased to low enough values, the disk mass is about 7 Jupiter mass which is enough to form a massive gaseous planet.

We thank the anonymous referee for valuable suggestions, and W. Kley for useful discussions. This work is supported by NSFC(10778603), National Basic Research Program of China(2007CB4800).

## A. APPENDIX

### A.1. Net Mass Accretion Ratio

For the sake of simplicity, colliding planetesimals, both the target and the projectile are normally considered as nearly homogeneous and spherical bodies, and all the collisions are treated as central impacts. Having these assumptions, to describe a specific collision needs only three input parameters: mass of target( $M_t$ ), mass of projectile( $M_p$ ), and impact velocity ( $V_{imp}$ , namely the  $\Delta V$  derived from our simulations).

Given a target and projectile of mass and radius  $M_t, R_t$  and  $M_p, R_p$  respectively, the surface escape velocity of the pair is

$$V_{esc}^2 = \frac{2G(M_t + M_p)}{(R_t + R_p)}, \quad (\text{A1})$$

Where  $G$  is the constant of gravity. The center of mass impact energy available for fragmentation is given by

$$Q_f = \frac{k_1}{2} V_{imp}^2 M_t M_p / (M_t + M_p), \quad (\text{A2})$$

where the impact efficiency  $k_1 = 0.5$  is the fraction of the impact energy not lost to heating. Assuming the crushing strength scaled by Love and Ahren (1996)

$$Q_c = 24.2 [R_t(\text{cm})]^{1.13}, \quad (\text{A3})$$

where  $R_t$  is the radius of the target in cm, then the mass of material fragmented by the impact is

$$M_f = Q_f / Q_c. \quad (\text{A4})$$

As some fragments fall back on the target by the gravity, the mass of material to escape is only a fraction of  $M_f$  and given by

$$M_e = k_2 M_f V_{esc}^{-2.25} \quad (\text{A5})$$

(Greenberg et al. 1978), where  $k_2 = 3 \times 10^6 \text{ (cm s}^{-1}\text{)}^{2.25}$ . Here in this paper, we define a ratio as being

$$A_r = 1 - M_e / M_p, \quad (\text{A6})$$

to measure the fraction of mass accreted on the target. If the derived  $M_e \geq M_p$  there is no growth of the target, and  $A_r = 0$  is forced in such cases. Figure 9 maps the  $A_r$  in the  $R_1$ - $R_2$  plane with four typical impact velocities: 100m/s, 300m/s, 600m/s, 1000m/s. As shown in figure 9, bodies with radius below 5 km hardly accrete each other, on the other hand, once one of the two colliding bodies has radius larger than 15 km, accretion is always efficient.

## REFERENCES

- Adachi, I., Hayashi, C., & Nakazawa, K. 1976, *Prog. Theor. Phys.*, 56, 1756
- Alexander, R. D., Clarke, C. J., Pringle, J. E. 2006a, *MNRAS*, 369, 216
- Alexander, R. D., Clarke, C. J., Pringle, J. E. 2006b, *MNRAS*, 369, 229
- Armitage, P. J. 2007, Lecture note on the formation and evolution of planetary systems, Preprint (astro-ph/0701485)
- Artymowicz, P. & Lubow, S.H. 1994, *AJ* 421, 651
- Barge, P., & Pellat, R. 1993, *Icarus*, 104, 79
- Bouwman, J., Lawson, W. A., Dominik, C., Feigelson, E. D., Henning, Th., Tielens, A. G. G. M., Waters, L. B. F. M. 2006, *ApJ*, 653, L57
- Brahic, A. 1977, *A&A*, 54, 895
- Chambers, J. E., & Wetherill, G. W. 1998, *Icarus*, 136, 304
- Charnoz, S., & Brahic, A. 2001b, *A&A*, 375, L31
- Charnoz, S., Thebault, P., & Brahic, A. 2001a, *A&A*, 373, 683
- Chen, C. H., & Kamp, I. 2004, *ApJ* 602, 985
- Durisen, R. H., Cai, K., Mejia, A. C., & Pickett, M. K. 2005, *Icarus*, 173, 417
- Goldreich, P., & Ward, W. R. 1973, *ApJ*, 183, 1051
- Greenberg, R., Hartmann, W. K., Chapman, C. R., Wacker, J. F. 1978, *Icarus*, 35, 1
- Haghighipour, N., & Boss, A. P. 2003, *ApJ*, 598, 1301
- Haisch, K. E., Lada, E. A., & Lada, C. J. 2001, *ApJ* 553, L153
- Hale, A. 1994, *AJ*, 107, 306
- Hartmann, L., Calvet, N., Gullbring, E., D'Alessio, P. 1998, *ApJ*, 495, 385
- Hatzes, A.P., Cochran, W.D., Endl, M., McArthur, B., Paulson, D., Walker, G.A.H., Campbell, B., & Yang, S. 2003, *ApJ*, 599, 1383
- Hayashi, C. 1981, *PthPS*, 70, 35

- Heppenheimer, T. A. 1978, *A&A*, 65, 421
- Hollenbach, D., Johnstone, D., Lizano, S., Shu, F. 1994, *ApJ*, 428, 654
- Hollenbach, D., Yorke, H.W., & Johnstone, D. 2000, in *Protostars and Planets IV*, ed. V. Mannings, A. P. Boss, & S. S. Russell (Tucson: Univ. Arizona Press), 401
- Kley, W., & Nelson, R. 2007, *On the Formation and Dynamical Evolution of Planets in Binaries*, preprint (astro-ph/07053421)
- Kokubo, E. & Ida, S. 1996, *Icarus*, 123, 180
- Kokubo, E. & Ida, S. 1998, *Icarus*, 131, 171
- Kokubo, E. & Ida, S. 2000, *Icarus*, 143, 15
- Kokubo, E., Kominami, J., Ida, S. 2006, *ApJ*, 642, 1131
- Kokubo, E., Yoshinaga K., & Makino, J. 1998, *MNRAS*, 297, 1067
- Kortenkamp, S. J., Wetherill, G. W. 2000, *Icarus*, 143, 60
- Levison, H. F., & Agnor, C. 2003, *AJ*, 125, 2692
- Lissauer, J. J. 1993, *ARA&A*, 31, 129
- Lithwick, Y., Chiang, E. 2007, *ApJ*, 656, 524
- Love, S. G., & Ahrens, T. J. 1996, *Icarus*, 124, 141
- Lynden-Bell, D., & Pringle, J. E. 1974, *MNRAS*, 168, 603
- Makino, J., Fukushige, T., Funato, Y., Kokubo, E. 1998, *New Astronomy*, 3, 411
- Marzari, F. & Scholl, H. 2000, *ApJ*, 543, 328
- Matsuyama, I., Johnstone, D., & Hartmann, L. 2003, *ApJ*, 582, 893
- Papaloizou, J. C. B., Terquem, C. 2006, *Rep. Prog. Phys.*, 69, 119
- Rafikov, R. R. 2003, *AJ*, 125, 942
- Rafikov, R. R. 2004, *AJ*, 128, 1348
- Rice, W. K. M., Lodato, G., Pringle, J. E., Armitage, P. J., & Bonnell, I. A. 2004, *MNRAS*, 355, 543

- Scholl, H., Marzari, F., Thbault, P. 2007, MNRAS, 380, 1119
- Strom, S. E., Edwards, S., & Skrutskie, M. F. 1993, in Protostars and Planets III, ed. E. H. Levy & J. I. Lunine (Tucson: Univ. Arizona Press), 837
- Thebault, P., Brahic, A. 1998, P&SS, 47, 233
- Thebault, P., Marzari, F., Scholl, H., Turrini, D., & Barbieri, M. 2004, A&A, 427, 1097
- Thebault, P., Marzari, F., & Scholl, H. 2006, Icarus, 183, 193
- Weidenschilling, S. J., & Cuzzi, J. N. 1993, in Protostars and Planets III, ed. E. H. Levy & J. I. Lunine (Tucson: Univ. Arizona Press), 1031
- Weidenschilling, S. J. 1997, ASPC, 122, 281
- Weidenschilling, S. J. & Davis, D. R. 1985, Icarus, 62, 16
- Wetherill, G. W., Stewart, G. R. 1989, Icarus, 77, 330
- Whitmire, D. P., Matese, J. J. & Criswell L. 1998, Icarus, 132, 196
- Youdin, A. N., & Chiang, E. 2004, ApJ, 601, 1109
- Youdin, A. N., & Shu, F. 2002, ApJ, 580, 494

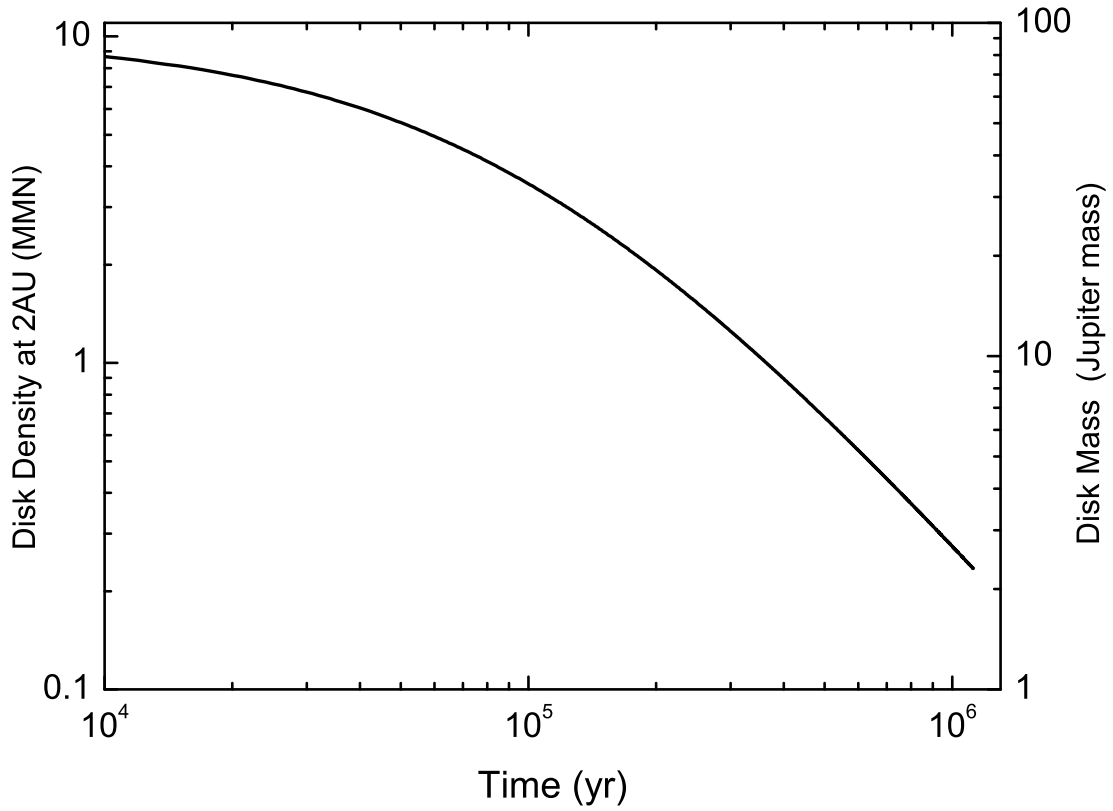


Fig. 1.— Gas disk dissipation with time. This curve is derived from Eq.(3). The left y-axis is the gas density at 2 AU with a initial value  $\rho_{g20} = 2 \times 10^{-9} \text{g cm}^{-3}$  (about 10 MMN), and the right one is the corresponding disk mass in Jupiter mass units. The mass of 1 MMN disk is estimated as 10 Jupiter mass roughly.

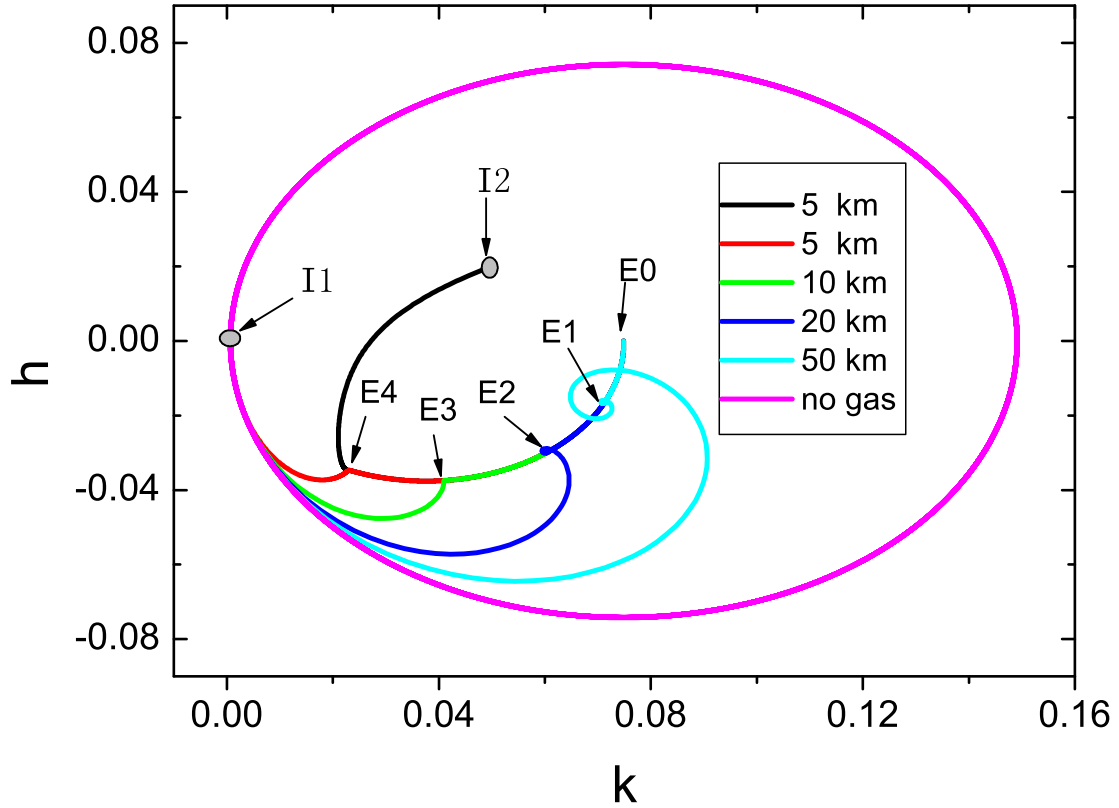


Fig. 2.— Phase diagram in  $h$ - $k$  plane. Gas disks are included for all the cases, except for the one denoted by the circle.  $E0$  is the equilibrium point without gas, while  $E1, E2, E3, E4$  are the equilibrium points for bodies of 50, 20, 10, 5 km respectively. All the motions are initially at point  $I1$  ( $h=k=0$ ), except for the black one that comes from point  $I2$ .

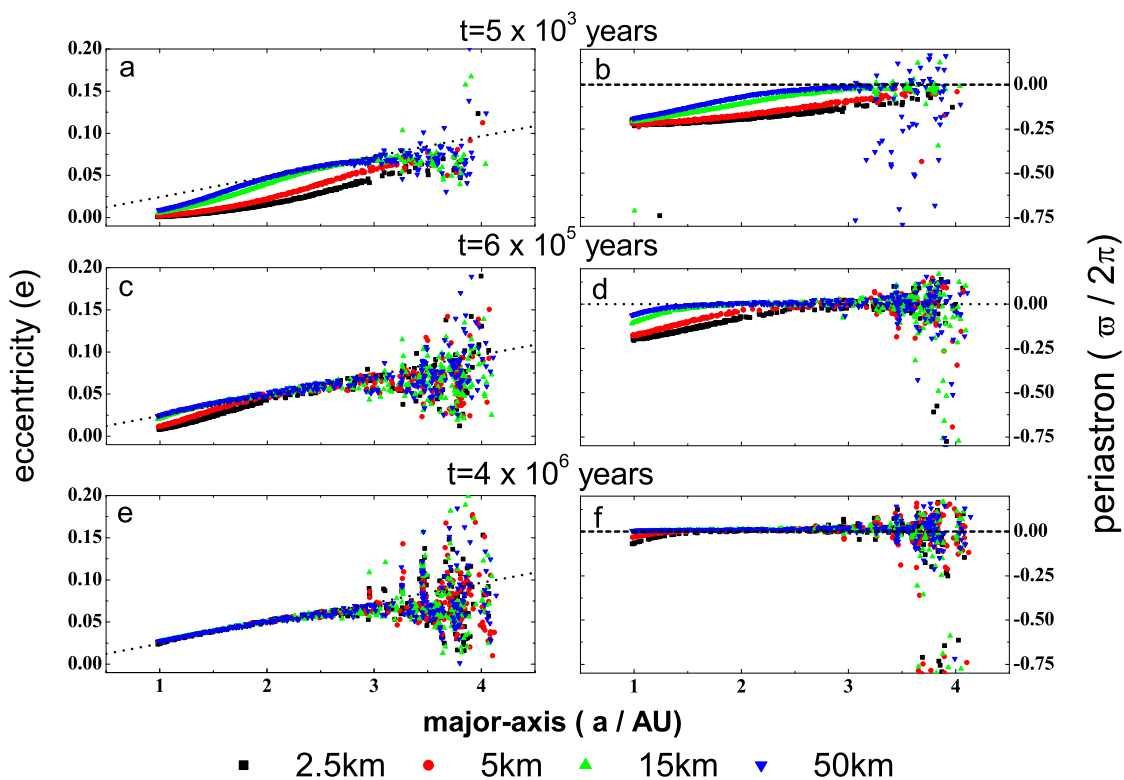


Fig. 3.— Distributions of planetesimal eccentricities and periastrons vs. semi-major axes at three different epochs. Bodies of different sizes are plotted in different styles. The dashed lines in the 3 left panels and 3 right ones denote  $e_f$  (forced eccentricity) and  $\varpi = 0$  (which means the planetesimal periastrons  $\varpi_p = \varpi_f$  the forced periastron), respectively.

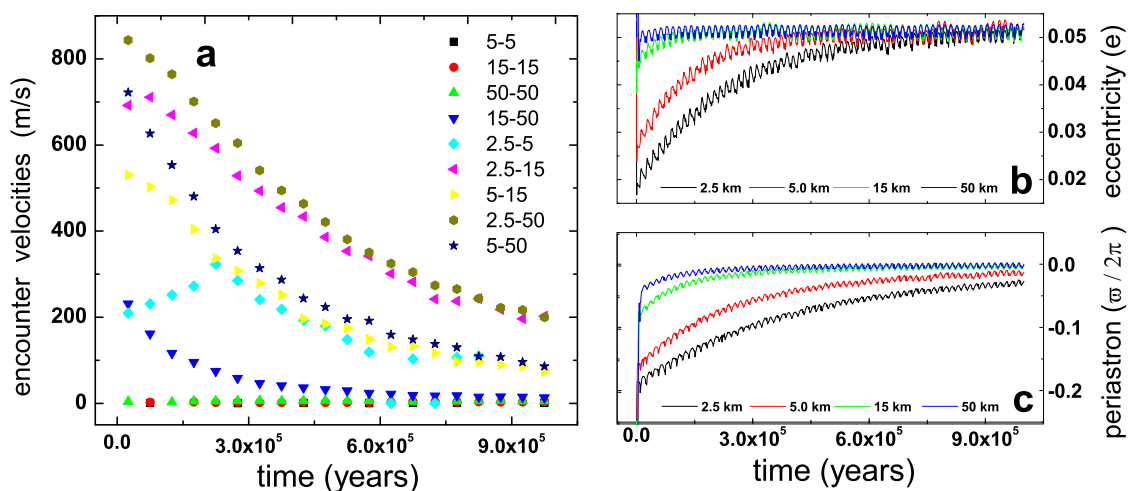


Fig. 4.— Time-evolutions of  $\Delta V$  and distributions of orbital elements at 2 AU from the star. (a) Average encounter velocities  $\Delta V$  at 2 AU from the primary star v.s. time in dissipating gas case.  $\Delta V$  between bodies of different sizes are plotted in different styles. (b) and (c): Average eccentricity and periastron( $\varpi$ ) at 2 AU from the primary v.s. time in dissipating gas case. Bodies of different sizes are plotted in different styles

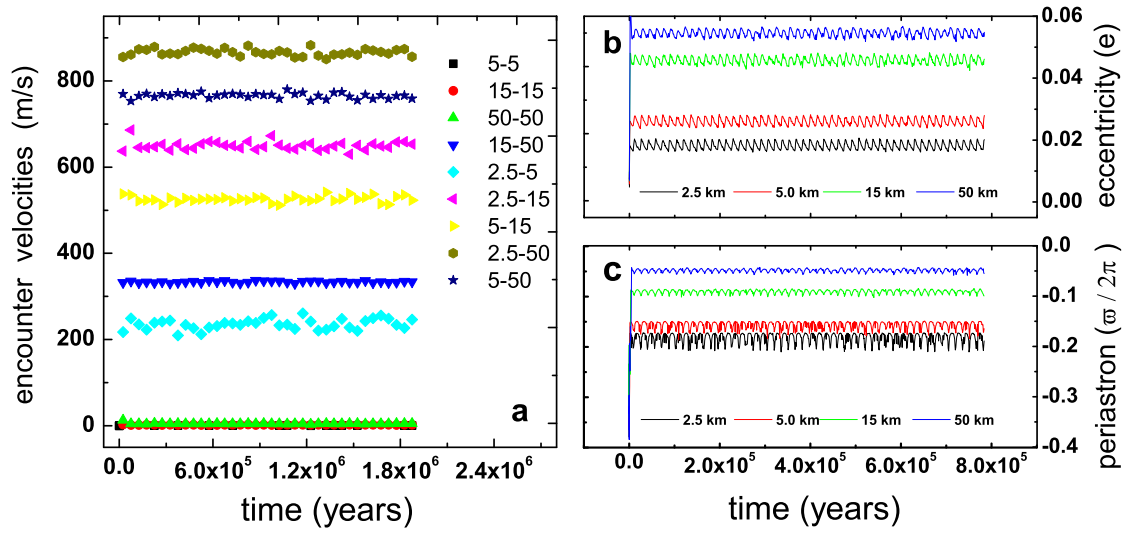


Fig. 5.— Same with figure 4 but for constant gas case

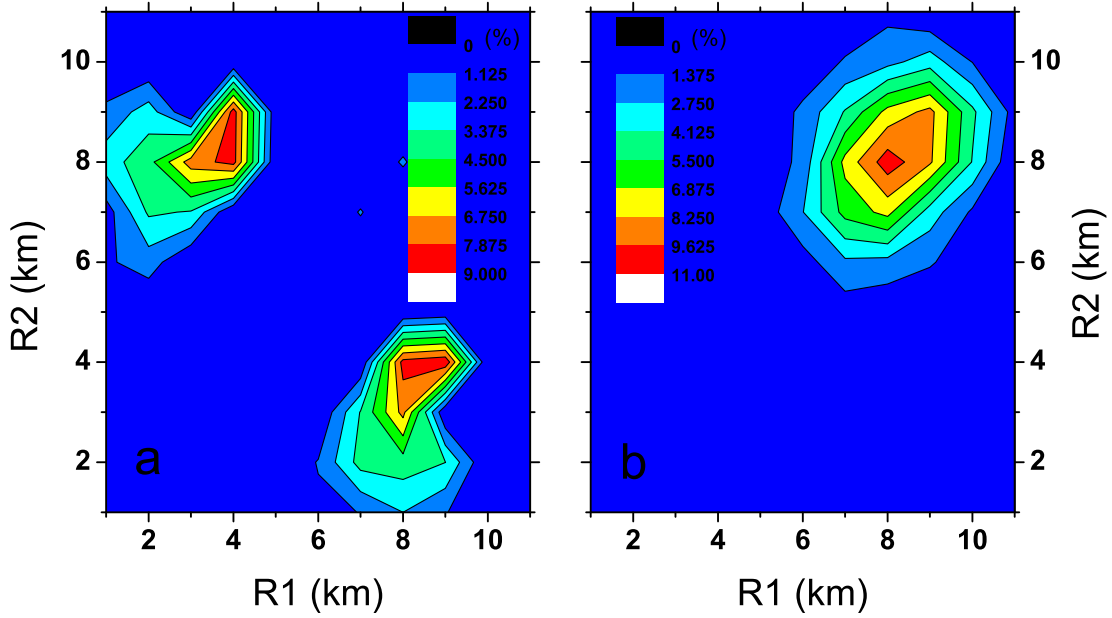


Fig. 6.— Distributions of impact rates in R1-R2 plane. R1, R2 are the radiuses of the two colliding bodies. The impact rates are computed as percentages of impacts that occur in areas of a given size in the R1-R2 plane. a: the case similar to that in figure 4, in which gas drag and companion’s perturbations are included. b: a case for compare, in which planetesimal eccentricities and periastrons are random, and gas drag and companion’s perturbations are not include (otherwise orbital elements will not be random any more) For both cases, a Gaussian size distribution, centered on  $R_p = 8\text{km}$ , is assumed for the size distribution of planetesimals.

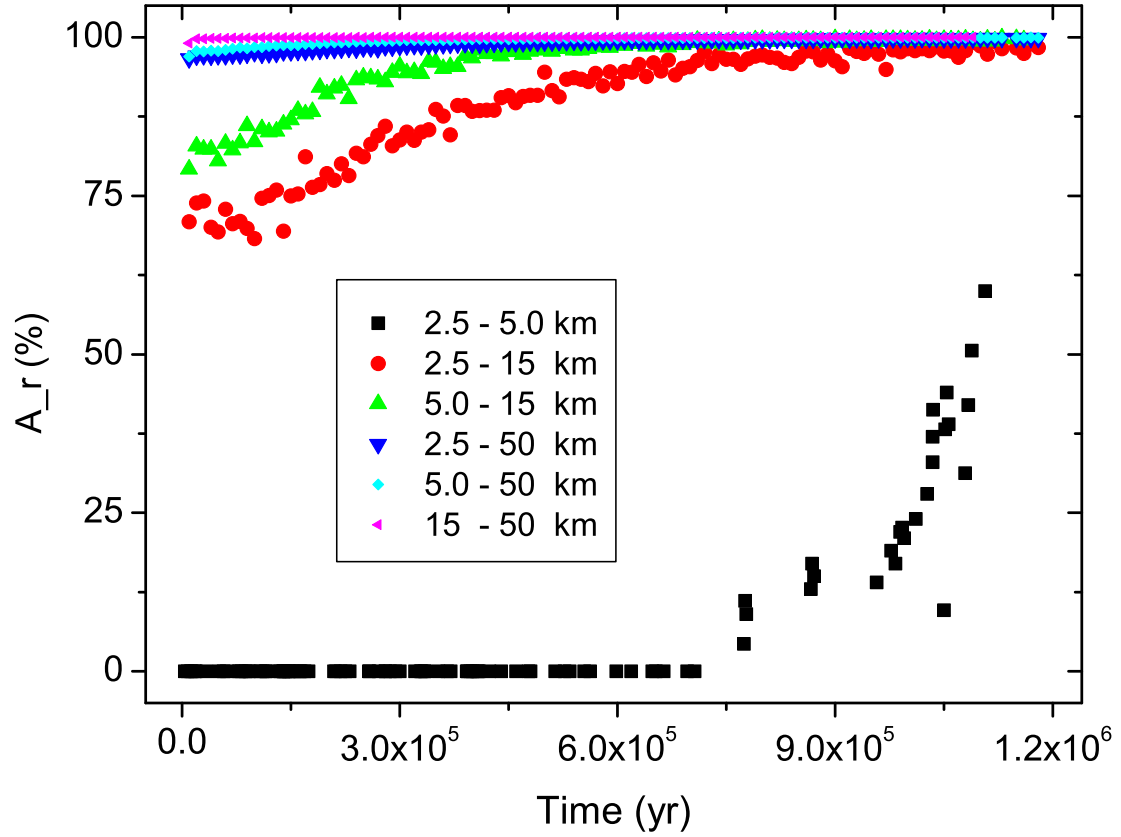


Fig. 7.— Time-evolutions of net mass accretion ratios for impacts between bodies of different sizes. Different types of impacts are plotted in different styles. The net mass accretion rates ( $A_r$ ) are defined and computed following the procedure described in the Appendix

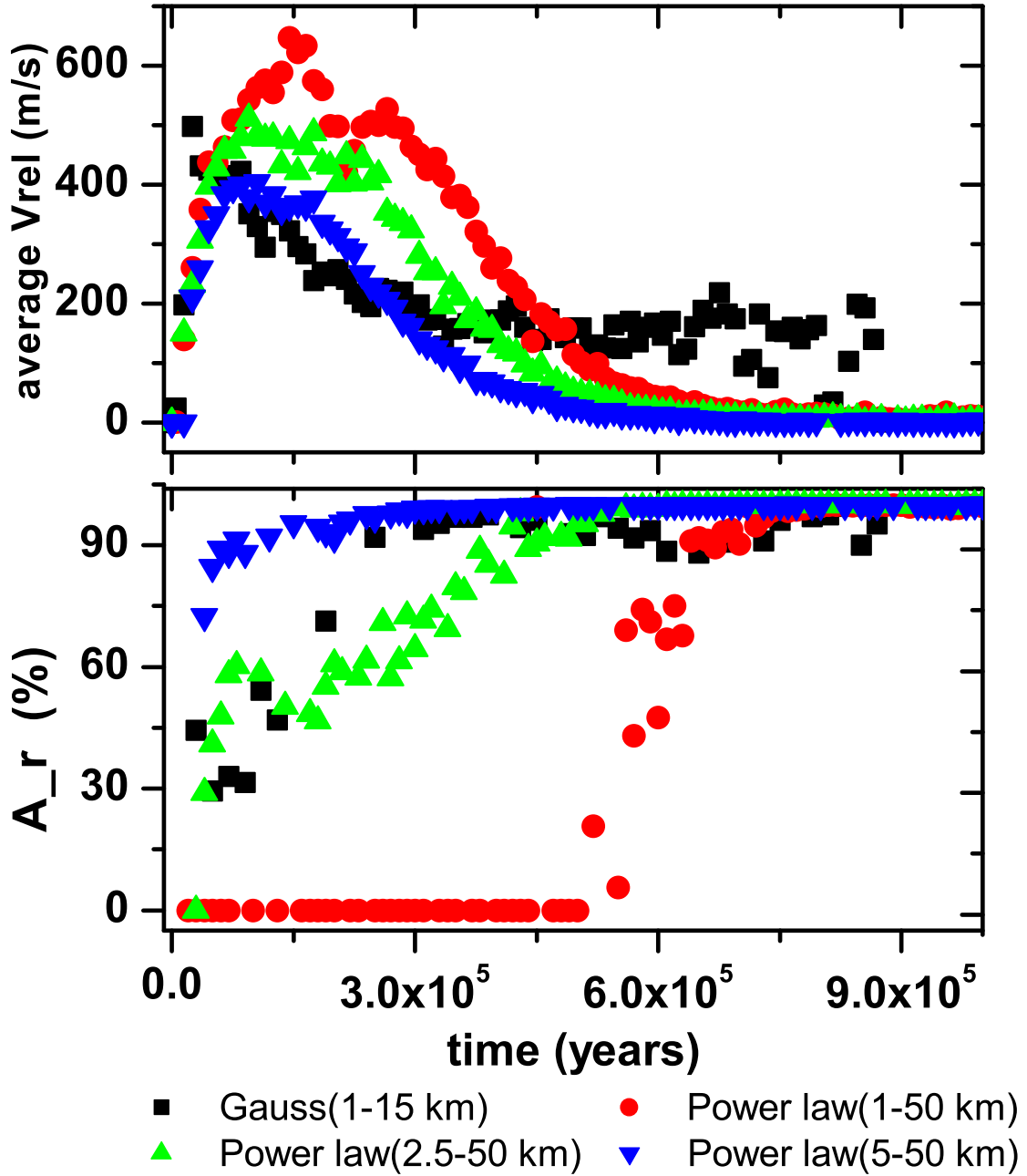


Fig. 8.— Correlation between net mass accretion ratio and the average relative velocity ( $\Delta V$ ), a: time evolution of  $\Delta V$ , b: time evolution of net mass accretion ratio. Cases with different size distributions are plotted in different styles. The net mass accretion rates ( $A_r$ ) are defined and computed following the procedure described in the Appendix

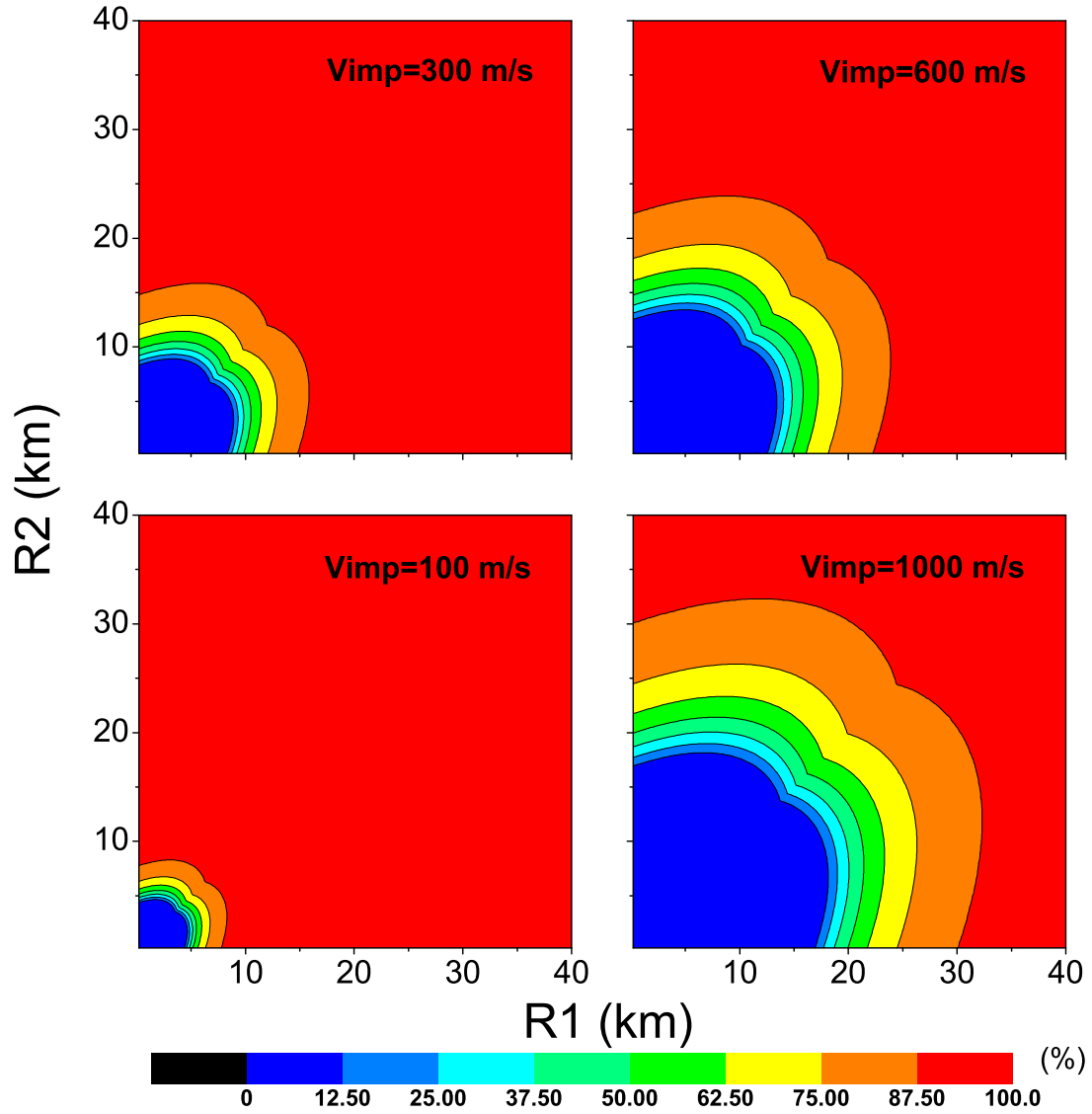


Fig. 9.— Net mass accretion ratios distributed in  $R1$ - $R2$  plane for 4 typical relative velocities: 100m/s, 300m/s, 600m/s, and 1000m/s.  $R1$ ,  $R2$  are the radiuses of the two colliding bodies. The net mass accretion rates are defined and computed following the procedure described in the Appendix

Table 1: Initial Parameters for Runs.

Parameters	Values	Units	Descriptions
$a_B$	18.5	$AU$	semi-major axis of companion
$e_B$	$0.361 \pm 0.023$	-	eccentricity of binary
$M_A$	1.6	$M_\odot$	mass of primary
$M_B$	0.4	$M_\odot$	mass of companion
$R_p$	2.5,5,15,50	$km$	physical radius of planetesimals
e	$0 \sim 0.1$	-	initial eccentricities of planetesimals
i	$0 \sim 10^{-3}$	-	initial inclinations of planetesimals
$\rho_p$	2.0	$g \cdot cm^{-3}$	planetesimal density
$\rho_{g20}$	$2 \times 10^{-9}$	$g \cdot cm^{-3}$	initial gas density at 2AU
$\rho_g$	$r^{-2.75}$	-	initial gas density radial profile

---

Note. —  $M_\odot$  stands for the solar mass